

# Comprehensive Study of Generalized Ghost Dark Energy in $f(Q, L_m)$ Gravity: New Insights into Cosmic Dynamics

M. Zeeshan Gul<sup>1,2\*</sup>, M. Sharif<sup>1†</sup>, Shan Ali Qureshi<sup>1‡</sup> and Baiju Dayanandan<sup>3 §</sup>

<sup>1</sup> Department of Mathematics and Statistics, The University of Lahore,  
1-KM Defence Road Lahore-54000, Pakistan.

<sup>2</sup> Research Center of Astrophysics and Cosmology, Khazar University,  
Baku, AZ1096, 41 Mehseti Street, Azerbaijan.

<sup>3</sup>Natural and Medical Sciences Research Center,  
University of Nizwa, Oman.

## Abstract

This paper explores the generalized ghost dark energy model in the framework of  $f(Q, L_m)$  gravity, where  $Q$  represents the non-metricity scalar and  $L_m$  denotes the matter-Lagrangian density. We take the homogeneous and isotropic universe with an ideal matter distribution and examine a scenario with interacting dark energy and dark matter. We then reconstruct  $f(Q, L_m)$  model to examine the effects of this extended gravitational framework on the cosmic evolution. The behavior of numerous cosmic parameters are explored corresponding to distinct parametric values. The stability is evaluated by the squared sound speed method. The statefinder  $(r, s)$  and standard diagnostic pairs  $(\omega_D - \omega'_D)$  are used to study the various cosmic eras. Our results

---

\*mzeeshangul.math@gmail.com, zeeshan.gul@khazar.org

†msharif.math@pu.edu.pk

‡shanali.math@gmail.com

§baiju@unizwa.edu.om

align with recent observational evidence, indicating that the  $f(Q, L_m)$  model effectively characterizes dark energy and cosmic evolution.

**Keywords:**  $f(Q, L_m)$  theory; Dark energy model; Cosmic evolution.

**PACS:** 95.36.+x; 98.80.-k; 04.50.Kd.

## 1 Introduction

The mysterious nature of the cosmos and astrophysical events has captivated numerous scholars to explore and study these phenomena. The cosmos consists of three major components, i.e., dark energy ( $DE$ ), dark matter ( $DM$ ) and normal matter. The universe is primarily governed by  $DE$  and  $DM$  with usual matter occupies the remaining space. The  $DM$  is an invisible matter and its existence is deduced by gravitational lensing and the rotation curves of galaxies [1]. However, the greatest ground-breaking finding of recent decades has been the accelerated expansion of the cosmos, which has steered scientific inquiry in a completely new direction. A mysterious source of energy which exhibits significant negative pressure, referred to as  $DE$  is thought to drive this expansion. The challenges surrounding the properties and existence of both  $DE$  and  $DM$  remain some of the complex and unsolved challenges in cosmology. The significant model for elucidating the characteristics of  $DE$  is the  $\Lambda$ CDM framework. In this model, the cosmological constant is regarded as the most probable explanation for the accelerating expansion of the universe. Although it aligns well with observational data, but it encounters challenges such as fine-tuning and the cosmic coincidence problem [2]. However, there are two methodologies to comprehend enigmatic features of the cosmos. One approach involves modifying the geometric aspect of the Einstein-Hilbert action, resulting in alternative theories of gravity, while the other focuses on altering the matter component to create dynamical  $DE$  models [3].

Researchers have proposed various methods to address these challenges in the past decades, yet they are still mysterious. To understand the nature of  $DE$ , the Veneziano ghost dark energy ( $GDE$ ) model has proposed in [4] which has notable physical effects. It generates a tiny vacuum energy density in curved spacetime corresponding to  $\Lambda_{QCD}^3$ , where  $QCD$  represents the quantum chromodynamics. Therefore, no additional parameters, degrees of freedom or alterations are needed. With  $\Lambda_{QCD} \sim 100 MeV$  and  $H \sim 10^{-33} eV$ ,

$\Lambda_{QCD}^3$  provides the proper order for the *DE* density. This shows that this paradigm eliminates the fine-tuning problem [5]. Cai et al [6] investigated the cosmic acceleration corresponding to *DE* model. Sheykhi and Movahed [7] examined cosmic evolution by analyzing the *GDE* model. The universe rapid growth via the *GDE* model has been investigated in [8].

Einstein's gravitational theory (*GR*) has been modified into various alternative gravitational theories due to their significant interest in explaining the accelerated expansion of the universe. The equivalent geometric frameworks can be used to represent *GR*. The initial approach focuses on curvature with the absence of both torsion and non-metricity. The second is the teleparallel formalism, where both non-metricity and curvature are absent. An alternative representation is also possible in which gravitational effects are characterized through the non-metricity of the metric, which reflects variations in a vector's length as it undergoes parallel transport. The fundamental principle of teleparallel gravity is to substitute the spacetime metric with a set of tetrad vectors, which introduces torsion. Additionally, curvature is substituted with the torsion produced by the vierbein, which serves to characterize the gravitational influences in the cosmos [9]. Linder [10] introduced modified teleparallel gravity ( $f(\mathbb{T})$ ), where  $\mathbb{T}$  denotes the torsion scalar. Jimenez et al [11] introduced the concept of symmetric teleparallel gravity, known as  $f(Q)$  gravity. A lot of significant work has been done in this modified framework [12]-[18].

Another modified proposal is  $f(Q, T)$  theory, which has become subject of great interest in scientific community due to its crucial implications in the field of cosmology and astrophysics [20]-[31]. Alternative theories and observational constraints has been examined in [32]-[39] Myrzakulov et al [40] generalized the symmetric teleparallel theory by including the matter-Lagrangian in the action, known as  $f(Q, L_m)$  theory. An important aspect of this gravity is that the corresponding field equations are of second-order which make this theory distinct from  $f(R)$  gravity ( $R$  represents the curvature invariant), which employs fourth-order field equations. This modified proposal investigates its potential consequences, its consistency with present experimental evidence and determine its applicability to cosmological models. The  $f(Q, L_m)$  theory establishes a unique relationship between geometry and matter, garnering a profound interest because of its significant consequences in gravitational physics. This theory is studied to comprehend its theoretical implications and importance in astrophysical and cosmological evolution. This theory proposes that the incorporation of non-metricity and

the existence of matter sources provide a more comprehensive representation of gravitational connections.

This theory incorporates non-metricity in the gravitational action, introducing additional degrees of freedom that result in novel gravitational dynamics and cosmological solutions. Additionally, the dependence on the matter-Lagrangian allows this theory to effectively characterize the impact of matter composition on the gravitational field. The objective of this modified theory is to provide a comprehensive framework for gravitational physics and cosmology, which can provide information about basic investigations into the nature of gravity and the cosmos. Harko et al [41] investigated diverse cosmological applications by deriving evolution equations and using particular functional forms for  $f(Q)$  gravity. Mandal and Sahoo [42] analyzed the equation of state (*EoS*) parameter in the framework of non-minimally coupled  $f(Q)$  gravity. Myrzakulov et al [43] further investigated the impact of bulk viscosity on late-time cosmic acceleration in  $f(Q, L_m)$  gravity framework.

The accelerated expansion of the universe can be examined using various *DE* models. Turner and White [44] found that the inflationary phase was not aligned with the present matter density and they tackled this problem by introducing a parameterization technique. Sahni et al [45] introduced a set of dimensionless diagnostic parameters to evaluate the characteristics of *DE*. Chirde and Shekh [46] used *DE* model and *EoS* parameter to examine the cosmic acceleration in  $f(R, T)$  gravity ( $T$  is the energy-momentum tensor). Arora et al [47] explored late-time cosmology involving dust matter in  $f(Q, T)$  framework. Solanki et al [48] examined the characteristics of various cosmic parameters in  $f(Q)$  gravity to examine the dark universe. Mussatayeva et al [49] described various late-time cosmological phenomena in the  $f(Q)$  gravity.

Reconstruction method in extended gravitational theories provide an effective reflection to explain the current accelerated expansion. Ebrahimi and Sheykhi [50] examined the *GDE* model in the context of Brans-Dicke cosmology using the non-interaction scenario. Saaidi et al [51] used correspondence approaches to reconstruct  $f(R)$  gravity models. Jawad [52] studied the evolutionary paths of few cosmic factors using the concept of pilgrim *DE* in  $f(\mathbb{T}, \mathbb{T}_G)$  theory. Fayaz et al [53] studied the  $f(R, T)$  model in the context of the *GDE* model and examined the evolutionary picture of the universe. Sharif and Nawazish [54] modified the  $f(R)$  gravity model using the generalized ghost pilgrim *DE* model with Friedmann-Robertson-Walker (*FRW*) universe. They discovered that the non-interacting condition exhibits cosmic acceleration, which is characterized by the presence of a positive cur-

vature parameter. The progression of the universe across matter and *DE* eras has been studied in [55]. Zadeh et al [56] found that the particle perspective accurately characterizes the cosmic acceleration during late time. Ghaffari et al [57] used Tsallis generalized entropy to establish a holographic *DE* model in Brans-Dicke Theory. Huang et al [58] analyzed cosmic evolution through Tsallis holographic *DE* model. Odintsov et al [59] investigated distinct  $f(R, G)$  models to elucidate the successful manifestation of the *DE* model. Myrzakulov et al [60] used the pilgrim *DE* and *GDE* models to rebuild the  $f(Q)$  model. They discovered that the outcomes achieved closely reflect the observational data. The construction of different models and cosmological analysis corresponding to *DE* models has been established in [61]-[63].

To examine the dynamics of the universe, we reconstruct the  $f(Q, L_m)$  functional form using the *GGDE* model to analyze the dynamics of the cosmos. This article follows the given format. Section 2 presents the basis of  $f(Q, L_m)$  gravity. Then, we assess the influence of the connection among *DE* and cold *DM* using analysis of the redshift parameter. We also reconstruct  $f(Q, L_m)$  functional form by considering *GGDE* model. Section 3 focuses on examining the evolution of this notion using cosmographic analysis. We summarize our main findings in section 4.

## 2 $f(Q, L_m)$ Theory: Field Equations

We derive the equations of motion of  $f(Q, L_m)$  theory by variational principle in this section. A generalized form of Riemannian geometry was presented by Weyl [42] as a mathematical foundation for the description of gravitation in *GR*. In Riemannian geometry, parallel transport along a closed path preserves the vector length and direction. Weyl introduced a modification in which a vector undergoes changes in both direction and length while being transported in parallel along a closed path. The proposed modification introduces a novel vector field ( $A^\xi$ ) that defines the geometric features of Weyl geometry. The primary fields in Weyl space consist of the newly defined vector field and the metric tensor. The metric tensor establishes the spatial arrangement of spacetime by specifying distances and angles, while the vector field is introduced to accurately represent the variation in length during parallel transport. In a Weyl theory, the length changes as  $\delta\ell = \ell A_\xi \delta x^\xi$  when a vector size  $\ell$  is transported with an infinitesimal path  $\delta x^\xi$  [43]. This suggests that the change in the size of the vector is directly related to the coefficient

of connection, original length and the displacement along the trajectory.

The variation in the vector length is expressed as  $\delta\ell = \ell\Upsilon_{\xi\eta}\delta h^{\xi\eta}$ , where  $\delta h^{\xi\eta}$  is the area element and

$$\Upsilon_{\xi\eta} = \nabla_{\eta}A_{\xi} - \nabla_{\xi}A_{\eta}. \quad (1)$$

A spatial scaling length  $\hat{\ell} = v(x)\ell$  transforms the field equation  $\hat{A}_{\xi}$  to  $\hat{A}_{\xi} = A_{\xi} + (\ln v)_{,\xi}$ , whereas the conformal transformations modify the elements of metric tensor as  $\hat{g}_{\xi\eta} = v^2g_{\xi\eta}$  and  $\hat{g}^{\xi\eta} = v^{-2}g^{\xi\eta}$ , respectively. Among the fundamental characteristics of Weyl geometry, a semi-metric connection is defined as

$$\hat{\Gamma}_{\xi\eta}^{\vartheta} = \Gamma_{\xi\eta}^{\vartheta} + g_{\xi\eta}A^{\vartheta} - \delta_{\xi}^{\vartheta}A_{\eta} - \delta_{\eta}^{\vartheta}A_{\xi}, \quad (2)$$

where Christoffel symbol is represented by  $\Gamma_{\xi\eta}^{\vartheta}$ . The construction of a gauge covariant derivative is possible by assuming that  $\hat{\Gamma}_{\xi\eta}^{\vartheta}$  is symmetric. Using the covariant derivative, the expression for the Weyl curvature tensor is

$$\hat{\mathcal{S}}_{\xi\eta\vartheta\gamma} = \hat{\mathcal{S}}_{(\xi\eta)\vartheta\gamma} + \hat{\mathcal{S}}_{[\xi\eta]\vartheta\gamma}, \quad (3)$$

where

$$\hat{\mathcal{S}}_{[\xi\eta]\vartheta\gamma} = \mathcal{S}_{\xi\eta\vartheta\gamma} + 2\nabla_{\vartheta}A_{[\xi g_{\eta]}\gamma} + 2\nabla_{\gamma}A_{[\eta g_{\xi]}\vartheta} + 2A_{\vartheta}A_{[\xi g_{\eta]}\vartheta} + 2A_{\gamma}A_{[\eta g_{\xi]}\vartheta} - 2A^2g_{\vartheta[\xi g_{\eta]}\gamma}.$$

After first contraction of the Weyl tensor, we have

$$\hat{\mathcal{S}}_{\eta}^{\xi} = \hat{\mathcal{S}}_{\vartheta\eta}^{\vartheta\xi} = \mathcal{S}_{\eta}^{\xi} + 2A^{\xi}A_{\eta} + 3\nabla_{\eta}A^{\xi} - \nabla_{\xi}A^{\eta} + g_{\eta}^{\xi}(\nabla_{\vartheta}A^{\vartheta} - 2A_{\vartheta}A^{\vartheta}). \quad (4)$$

Finally, the Weyl scalar is given by

$$\hat{\mathcal{S}} = \bar{\mathcal{S}}_{\vartheta}^{\vartheta} = \mathcal{S} + 6(\nabla_{\xi}A^{\xi} - A_{\xi}A^{\xi}). \quad (5)$$

Weyl-Cartan (WC) spaces, which include torsion offer an expanded framework that goes beyond Riemannian and Weyl geometries.

The WC spacetimes are characterized by a symmetric metric tensor defining the length of a vector and an asymmetric connection determines the law of parallel transport as  $d\zeta^{\xi} = -\zeta^{\vartheta}\hat{\Gamma}_{\vartheta\eta}^{\xi}dx^{\eta}$  [59]. The connection in this framework is given by

$$\tilde{\Gamma}_{\xi\eta}^{\vartheta} = \Gamma_{\xi\eta}^{\vartheta} + \Psi_{\xi\eta}^{\vartheta} + \Omega_{\xi\eta}^{\vartheta}. \quad (6)$$

Here, disformation tensor ( $\Omega_{\xi\eta}^{\vartheta}$ ) and contortion tensor ( $\Psi_{\xi\eta}^{\vartheta}$ ) are expressed as

$$\Omega_{\xi\eta}^{\vartheta} = \frac{1}{2}g^{\vartheta\gamma}(Q_{\xi\eta\gamma} + Q_{\xi\eta\gamma} - Q_{\gamma\xi\eta}), \quad (7)$$

$$\Psi_{\xi\eta}^{\vartheta} = \tilde{\Gamma}_{[\xi\eta]}^{\vartheta} + g^{\vartheta\gamma}g_{\xi\varepsilon}\tilde{\Gamma}_{[\eta\gamma]}^{\varepsilon} + g^{\vartheta\gamma}g_{\eta\varepsilon}\tilde{\Gamma}_{[\xi\gamma]}^{\varepsilon}, \quad (8)$$

where

$$Q_{\gamma\xi\eta} = \nabla_{\gamma}g_{\xi\eta} = -g_{\xi\eta,\gamma} + g_{\eta\varepsilon}\hat{\Gamma}_{\xi\gamma}^{\varepsilon} + g_{\varepsilon\xi}\hat{\Gamma}_{\eta\gamma}^{\varepsilon}. \quad (9)$$

Here, *WC* connection is denoted by  $\tilde{\Gamma}_{\xi\eta}^{\vartheta}$ . It is noted that the *WC* geometry represents a specific case of Weyl geometry when torsion is absent as verified from Eqs.(2) and (6), where  $Q_{\vartheta\xi\eta} = -2g_{\xi\eta}\Psi_{\vartheta}$ . Therefore, Eq.(6) becomes

$$\tilde{\Gamma}_{\xi\eta}^{\vartheta} = \Gamma_{\xi\eta}^{\vartheta} + g_{\xi\eta}\Psi^{\vartheta} - \delta_{\xi}^{\vartheta}\Psi_{\eta} - \delta_{\eta}^{\vartheta}\Psi_{\xi} + \Psi_{\xi\eta}^{\vartheta}, \quad (10)$$

with

$$\Psi_{\xi\eta}^{\vartheta} = T_{\xi\eta}^{\vartheta} - g^{\vartheta\gamma}g_{\varepsilon\xi}T_{\gamma\eta}^{\varepsilon} - g^{\vartheta\gamma}g_{\varepsilon\eta}T_{\gamma\xi}^{\varepsilon}. \quad (11)$$

The *WC* torsion is given by

$$T_{\xi\eta}^{\vartheta} = \frac{1}{2}(\tilde{\Gamma}_{\xi\eta}^{\vartheta} - \tilde{\Gamma}_{\eta\xi}^{\vartheta}). \quad (12)$$

A connection-based definition of the *WC* curvature tensor is

$$\tilde{\mathcal{S}}_{\xi\eta\gamma}^{\vartheta} = \tilde{\Gamma}_{\xi\gamma,\eta}^{\vartheta} - \tilde{\Gamma}_{\xi\eta,\gamma}^{\vartheta} + \tilde{\Gamma}_{\xi\gamma}^{\varepsilon}\tilde{\Gamma}_{\varepsilon\eta}^{\vartheta} - \tilde{\Gamma}_{\xi\eta}^{\varepsilon}\tilde{\Gamma}_{\varepsilon\gamma}^{\vartheta}. \quad (13)$$

Contraction of the curvature tensor yields the *WC* scalar as

$$\begin{aligned} \tilde{\mathcal{S}} &= \tilde{\mathcal{S}}_{\xi\eta}^{\xi\eta} = \mathcal{S} + 6\nabla_{\eta}\Psi^{\eta} - 4\nabla_{\eta}T^{\eta} - 6\Psi_{\eta}\Psi^{\eta} + 8A_{\eta}T^{\eta} + T^{\xi\vartheta\eta}T_{\xi\vartheta\eta} \\ &+ 2T^{\xi\vartheta\eta}T_{\eta\vartheta\xi} - 4T^{\eta}T_{\eta}, \end{aligned} \quad (14)$$

where  $T_{\eta} = T_{\xi\eta}^{\xi}$ .

By neglecting the boundary terms in the Ricci scalar, one can reformulate the gravitational action as [50]

$$S = \frac{1}{2\kappa} \int g^{\xi\eta}(\Gamma_{\gamma\xi}^{\vartheta}\Gamma_{\vartheta\eta}^{\gamma} - \Gamma_{\gamma\vartheta}^{\vartheta}\Gamma_{\xi\eta}^{\gamma})\sqrt{-g}d^4x. \quad (15)$$

The assumption of symmetric connection yields

$$\Gamma_{\xi\eta}^{\vartheta} = -L_{\xi\eta}^{\vartheta}. \quad (16)$$

Thus, Eq.(15) turns out to be

$$S = -\frac{1}{2\kappa} \int g^{\xi\eta}(L_{\gamma\xi}^{\vartheta}L_{\vartheta\eta}^{\gamma} - L_{\gamma\vartheta}^{\vartheta}L_{\xi\eta}^{\gamma})\sqrt{-g}d^4x, \quad (17)$$

where

$$Q \equiv -g^{\xi\eta}(L_{\gamma\xi}^\vartheta L_{\vartheta\eta}^\gamma - L_{\eta\vartheta}^\vartheta L_{\xi\eta}^\eta), \quad (18)$$

and

$$L_{\gamma\xi}^\vartheta \equiv -\frac{1}{2}g^{\vartheta\varepsilon}(\nabla_\xi g_{\gamma\varepsilon} + \nabla_\gamma g_{\varepsilon\xi} - \nabla_\varepsilon g_{\gamma\xi}). \quad (19)$$

By substituting the non-metricity scalar with a general function in Eq.(17), the gravitational action of symmetric teleparallel theory can be derived as

$$S = \frac{1}{2\kappa} \int f(Q)\sqrt{-g}d^4x. \quad (20)$$

Now, we couple this action with the matter-Lagrangian density, the action of  $f(Q, L_m)$  theory is obtained as [6, ?]

$$S = \frac{1}{2\kappa} \int f(Q, L_m)\sqrt{-g}d^4x. \quad (21)$$

The superpotential is given by

$$\mathcal{P}_{\xi\eta}^\vartheta = -\frac{1}{2}L_{\xi\eta}^\vartheta + \frac{1}{4}(Q^\vartheta - \tilde{Q}^\vartheta)g_{\xi\eta} - \frac{1}{4}\delta_{[\xi}^\vartheta Q_{\eta]}. \quad (22)$$

The relation for non-metricity (given in Appendix  $\mathcal{X}$ ) is

$$Q = -Q_{\vartheta\xi\eta}\mathcal{P}^{\vartheta\xi\eta} = -\frac{1}{4}(-Q^{\vartheta\xi\eta}Q_{\vartheta\xi\eta} + 2Q^{\vartheta\xi\eta}Q_{\eta\vartheta\xi} - 2Q^\vartheta\tilde{Q}_\vartheta + Q^\vartheta Q_\vartheta). \quad (23)$$

The variation of Eq.(21) gives

$$\begin{aligned} \delta S &= \frac{1}{2} \int \delta[f(Q, L_m)\sqrt{-g}]d^4x, \\ &= \frac{1}{2} \int (f\delta\sqrt{-g} + (f_Q\delta Q + f_{L_m}\delta L_m)\sqrt{-g})d^4x. \end{aligned} \quad (24)$$

Moreover, we define

$$T_{\xi\eta} = -\frac{2}{\sqrt{-g}} \frac{\delta(\sqrt{-g}L_m)}{\delta g^{\xi\eta}} = g_{\xi\eta}L_m - 2\frac{\partial L_m}{\partial g^{\xi\eta}}. \quad (25)$$

The variation of  $Q$  is discussed in Appendix  $\mathcal{Y}$  and determinant of the metric tensor is given by

$$\delta\sqrt{-g} = -\frac{1}{2}\sqrt{-g}g_{\xi\eta}\delta g^{\xi\eta}. \quad (26)$$



Using Eqs.(25), (26) and variation of  $\delta Q$  in (24), we have

$$\begin{aligned}\delta S &= \frac{-1}{2} \int f g_{\xi\eta} \sqrt{-g} \delta g^{\xi\eta} \\ &- f_Q \sqrt{-g} (\mathcal{P}_{\xi\vartheta\gamma} Q_\eta^{\vartheta\gamma} - 2Q_\xi^{\vartheta\gamma} \mathcal{P}_{\vartheta\gamma\eta}) \delta g^{\xi\eta} + 2f_Q \sqrt{-g} \mathcal{P}_{\vartheta\xi\eta} \nabla^{\vartheta} \delta g^{\xi\eta} \\ &+ \frac{1}{2} f_{L_m} (L_m - \mathcal{T}_{\xi\eta}) \sqrt{-g} \delta g^{\xi\eta} d^4x.\end{aligned}\quad (27)$$

Integrate while considering the boundary conditions, the term  $2f_Q \sqrt{-g} \mathcal{P}_{\vartheta\xi\eta} \nabla^{\vartheta} \delta g^{\xi\eta}$  takes the form as  $-2\nabla^{\vartheta} (f_Q \sqrt{-g} \mathcal{P}_{\vartheta\xi\eta}) \delta g^{\xi\eta}$ . The resulting field equations of  $f(Q, L_m)$  gravity are

$$\begin{aligned}\frac{1}{2} f_{L_m} (L_m - \mathcal{T}_{\xi\eta}) &= \frac{2}{\sqrt{-g}} \nabla_{\vartheta} (f_Q \sqrt{-g} \mathcal{P}_{\xi\eta}^{\vartheta}) + \frac{1}{2} f g_{\xi\eta} \\ &+ f_Q (\mathcal{P}_{\xi\vartheta\gamma} Q_\eta^{\vartheta\gamma} - 2Q_\xi^{\vartheta\gamma} \mathcal{P}_{\vartheta\gamma\eta}),\end{aligned}\quad (28)$$

where  $f_{L_m} = \frac{\partial f}{\partial L_m}$  and  $f_Q = \frac{\partial f}{\partial Q}$ .

## 2.1 Formulation of *GGDE* $f(Q, L_m)$ Model

To explore the mysteries of the cosmos, we consider a homogeneous and isotropic spacetime characterized by the scale factor  $a(t)$  as

$$ds^2 = -dt^2 + a^2(t)(dx^2 + dy^2 + dz^2).\quad (29)$$

We assume that the universe is filled with ideal fluid, whose stress-energy tensor is expressed as

$$T_{\xi\eta} = (\mu + P)\mathcal{V}_\xi \mathcal{V}_\eta + P g_{\xi\eta},\quad (30)$$

where  $\mu$ ,  $P$  and  $\mathcal{V}_\xi$  represent the energy density, pressure and four-velocity of the fluid, respectively. The non-zero components of the non-metricity and deformation tensor are

$$\begin{aligned}Q_{011} &= Q_{022} = Q_{033} = 2a\dot{a}, \\ Q_0^{11} &= Q_0^{22} = Q_0^{33} = \frac{2\dot{a}}{a^3}, \\ Q^{01}{}_{1} &= Q^{02}{}_{2} = Q^{03}{}_{3} = -\frac{2\dot{a}}{a},\end{aligned}$$

$$\begin{aligned}
L^0_{11} &= L^0_{22} = L^0_{33} = -a\dot{a}, \\
L^1_{01} &= L^1_{10} = L^2_{02} = L^2_{20} = L^3_{03} = L^3_{30} = -\frac{\dot{a}}{a}.
\end{aligned}$$

Using the values of these non-zero components with flat *FRW* spacetime in Eq.(23), we have

$$\begin{aligned}
P^0_{11} &= P^0_{22} = P^0_{33} = -a\dot{a}, \\
P^{011} &= P^{022} = P^{033} = -\frac{\dot{a}}{a^3}, \\
P_{011} &= P_{022} = P_{033} = a\dot{a}, \\
P^1_{01} &= P^0_{10} = P^2_{02} = P^2_{20} = P^3_{03} = P^3_{30} = -\frac{\dot{a}}{4a}, \\
P_{110} &= P_{101} = P_{220} = P_{202} = P_{330} = P_{303} = -\frac{a\dot{a}}{4}, \\
P^{110} &= P^{101} = P^{220} = P^{202} = P^{330} = P^{303} = -\frac{\dot{a}}{4a^3}.
\end{aligned}$$

The non-metricity scalar is calculated by using Eq.(25) as

$$Q = -(Q_{011}P^{011} + Q_{022}P^{022} + Q_{033}P^{033}).$$

After simplifying this equation, we obtain  $Q = 6H^2$ , where  $H = \frac{\dot{a}}{a}$ . Evaluating Eq.(29) for 0-0 component, we have

$$\frac{2}{a^3}\nabla_\mu(f_Q\sqrt{-g}P^\mu_{00}) + f_Q(P_{0\mu\nu}Q_0{}^{\mu\nu} - 2Q^{\mu\nu}{}_0P_{\mu\nu 0}) + \frac{1}{2}fg_{00} = \frac{1}{2}f_{L_m}(g_{00}L_m - T_{00}).$$

This equation turns out to be

$$f_Q(P_{011}Q_0{}^{11} + P_{022}Q_0{}^{22} + P_{033}Q_0{}^{33}) - \frac{1}{2}f = \frac{1}{2}f_{L_m}(\rho + L_m).$$

After simplification, we have

$$3H^2 = \frac{1}{4f_Q}(f - f_{L_m}(\mu + L_m)). \quad (31)$$

Equation (29) for the 1-1 component becomes

$$\frac{2}{a^3}\nabla_\mu(f_Q\sqrt{-g}P^\mu_{11}) + f_Q(P_{1\mu\nu}Q_1{}^{\mu\nu} - 2Q^{\mu\nu}{}_1P_{\mu\nu 1}) + \frac{1}{2}fg_{11} = \frac{1}{2}f_{L_m}(g_{11}L_m - T_{11}).$$

Manipulation of this equation yields

$$\frac{2}{a^3} \frac{\partial}{\partial t} (f_Q a^3 (-a\dot{a})) - 4\dot{a}^2 f_Q + \frac{a^2}{2} \dot{f} = \frac{a^2}{2} f_{L_m} (L_m - p).$$

Rearranging this equation, we have

$$\dot{H} + 3H^2 + \frac{\dot{f}_Q}{f_Q} H = \frac{1}{4f_Q} (f + f_{L_m} (\mu - L_m)), \quad (32)$$

where dot represents the temporal derivative,  $\mu_D$  and  $P_D$  represent the energy density and pressure corresponding to  $DE$  expressed as

$$\mu_D = \frac{-12H^2 f_Q - L_m f_{L_m} + f}{f_L}, \quad (33)$$

$$P_D = \frac{4(\dot{L}_m H f_{QL} + 3H^2 (4\dot{H} f_{QQ} + f_Q) + \dot{H} f_Q) + L_m f_{L_m} - f}{f_{L_m}}. \quad (34)$$

The relations for the fractional energy densities are specified as follows

$$\Omega_D = \frac{\mu_D}{3H^2}, \quad \Omega_m = \frac{\mu_m}{3H^2}, \quad (35)$$

This implies that  $1 = \Omega_D + \Omega_m$ , indicating the interplay between  $DE$  and  $DM$ . Consequently, the conservation of energy densities for two fluids can be determined as follows when they interact

$$\dot{\mu}_m + 3H(\mu_m + P_m) = \Gamma, \quad \dot{\mu}_D + 3H(\mu_D + P_D) = -\Gamma. \quad (36)$$

Here,  $\Gamma$  is the interaction term. The interaction term must be positive for energy transfer from  $DE$  to  $DM$ . In this specific framework, we examine the equation  $\Gamma = 3\eta H(\mu_m + \mu_D) = 3H\eta\mu_D(1 + \beta)$ , where  $\eta$  defines the coupling constant and  $\beta$  is given by

$$\beta = \frac{\mu_m}{\mu_D} = \frac{\Omega_m}{\Omega_D} = \frac{1 - \Omega_D}{\Omega_D}. \quad (37)$$

We can express the  $\omega_D$  as

$$\omega_D = -\frac{2\eta + 1}{2 - \Omega}. \quad (38)$$

The dynamic  $DE$  models that incorporate direct relation between energy density and the Hubble parameter is crucial for elucidating the phenomenon

of the accelerated expansion of the universe. In this context, the energy density of the *GGDE* model is represented as

$$\mu_D = \alpha H + \beta H^2. \quad (39)$$

Using Eqs.(33) and (39), we have

$$\frac{-12H^2 f_Q - L_m f_L + f}{f_L} = \alpha H + \beta H^2. \quad (40)$$

We consider  $L_m = p$  and use Eq.(36), we obtain the reconstructed *GGDE*  $f(Q, L_m)$  model as

$$f(Q, L_m) = -\frac{\alpha c_1 \sqrt{Q}(\ln(Q) + 2)}{2\sqrt{6}} - \frac{1}{3}\beta c_1 Q, \quad (41)$$

where  $c_1$  is the integration constant. Substituting this reconstructed functional form in Eqs.(33) and (34), we have

$$\mu_D = \frac{\sqrt{6}\alpha(6H^2(\ln(Q) + 2) - Q\ln(Q)) - 2\beta\sqrt{Q}(Q - 12H^2)}{12\sqrt{Q}}, \quad (42)$$

$$P_D = \frac{1}{12Q^{3/2}}(2\beta Q^{3/2}(-4\dot{H} - 12H^2 + Q) + \sqrt{6}\alpha(Q(Q\ln(Q) - 2(\ln(Q) + 2)\dot{H}) - 6H^2(Q(\ln(Q) + 2) - 2\ln(Q)\dot{H}))). \quad (43)$$

Now, we examine the cosmic parameters through the redshift function, which is significant to comprehend the dynamics and the evolution of the universe. The dynamics of redshift provides insights on cosmic acceleration and the motion of cosmic objects with time. In this perspective, we consider the scale factor as

$$a(t) = a_0 t^k, \quad (44)$$

where  $a_0$  and  $k$  are arbitrary constants. The deceleration parameter is represented as

$$q = -\frac{a\ddot{a}}{\dot{a}^2} = -1 + \frac{1}{k}. \quad (45)$$

This is a crucial cosmographic parameter that demonstrates the rate of the expanding universe, because the cosmos undergoes decelerated expansion for positive values of deceleration parameter, whereas its negative values signify accelerated cosmic expansion. By using the value of  $k$ , Eq.(44) becomes

$$a(t) = t^{\frac{1}{1+q}}, \quad (46)$$

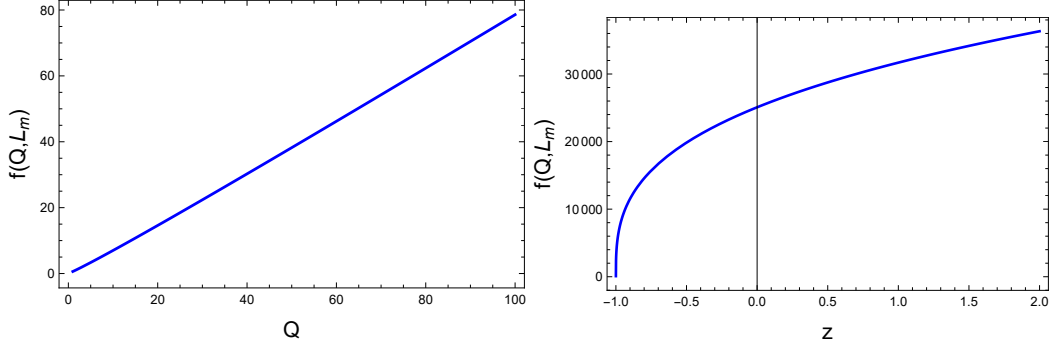


Figure 1: Graph of  $f(Q, L_m)$  versus non-metricity and redshift for  $\alpha = 1.5$ ,  $\beta = 6.5$  and  $c_1 = 0.4$ .

where the present deceleration parameter value is  $q = -0.832^{+0.091}_{-0.091}$  [64]. The relation for  $H$  and  $H_0$  is represented as

$$H = \frac{\dot{a}}{a} = \left( \frac{1}{1+q} \right) \left( \frac{1}{t} \right), \quad H_0 = \left( \frac{1}{1+q} \right) \left( \frac{1}{t_0} \right). \quad (47)$$

This signifies that the universe expansion is impacted by the deceleration parameter and  $H_0$ . By computing the correlation between the redshift parameter and the scale factor, we have

$$H = H_0 \mathcal{U}^{1+q}, \quad \dot{H} = -H_0 \mathcal{U}^{2+2q}, \quad (48)$$

where  $\mathcal{U} = 1 + z$  [65]. The non-metricity term is given by

$$Q = 6H_0^2 \mathcal{U}^{2+2q}. \quad (49)$$

We consider Substituting these values in Eq.(41), we get

$$\begin{aligned} f(Q, L_m) &= -\frac{1}{2} \alpha c_1 \sqrt{H_0^2 \mathcal{U}^{2q+2} (\log(6H_0^2 \mathcal{U}^{2q+2}) + 2)} \\ &\quad - 2\beta c_1 H_0^2 \mathcal{U}^{2q+2}. \end{aligned} \quad (50)$$

Figure 1 demonstrates that the reconstructed  $f(Q, L_m)$  model retains a positive value and exhibits an increasing trend corresponding to both redshift function and non-metricity scalar. This graphical analysis indicates that the reconstructed *GGDE* model supports the cosmic acceleration. It is noteworthy that as  $Q$  approaches to zero, our rebuilt model converges to zero,

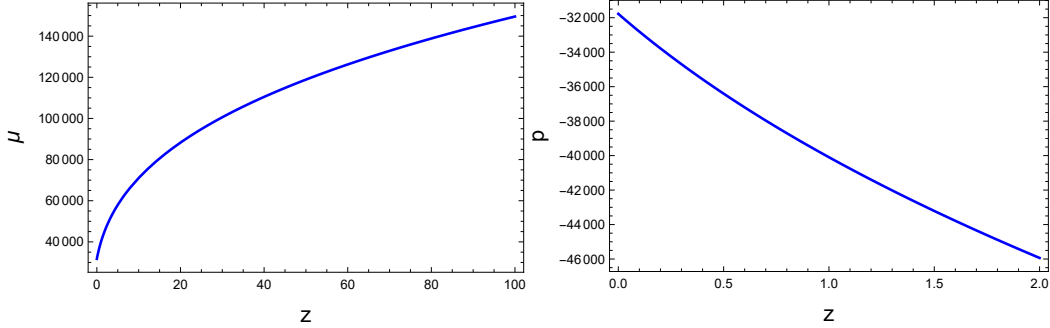


Figure 2: Graphical representation of matter variables versus redshift for  $\alpha = 1.5$ ,  $\beta = 6.5$  and  $c_1 = 0.4$ .

signifying that the reconstructed model exhibits realistic behavior. Substituting Eq.(49) in (42) and (43), we have

$$\mu_D = \alpha \sqrt{H_0^2 \mathcal{U}^{2q+2} + \beta H_0^2 \mathcal{U}^{2q+2}}, \quad (51)$$

$$P_D = -\alpha \sqrt{H_0^2 \mathcal{U}^{2q+2} - \beta H_0^2 \mathcal{U}^{2q+2}}. \quad (52)$$

In cosmology, the composition of matter offers significant insights into the cosmic evolution. Figure 2 determines the graphical behavior of energy density and pressure corresponding to reconstructed *GGDE*  $f(Q, L_m)$ . As observed from these plots, the pressure remains negative and the energy density is positive. These graphical behaviors align with the characteristics of *DE*, suggesting accelerated expansion. The distinct behaviors of energy density and pressure help to evaluate the viability of this bouncing model, underscoring its relevance in advancing our understanding of cosmic evolution.

### 3 Study of Cosmographic Parameters

This section examines the dynamics of the cosmos through cosmographic analysis of the key cosmic parameters for the reconstructed *GGDE*  $f(Q, L_m)$  framework. Moreover, we examine consistency of this model using the sound speed approach.

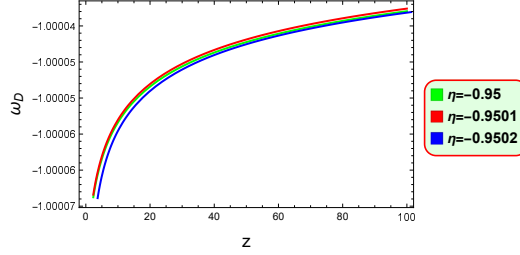


Figure 3: Graph of  $\omega_D$  versus redshift for  $\alpha = 1.5$ ,  $\beta = 6.5$  and  $c_1 = 0.4$ .

### 3.1 Analysis of State Parameter

The *EoS* parameter ( $\omega = \frac{P}{\mu}$ ) represents correlation between energy density and pressure. This parameter helps to comprehend how these components impact cosmic dynamics. This parameter sheds light on the forces driving cosmic evolution and provides a more detailed understanding of the universe progression. Different values of  $\omega$  correspond to various cosmic epochs, it distinguishes between different expansion phases, where  $\omega \in (-1, -\frac{1}{3})$  corresponds to quintessence era and  $\omega \in (-\infty, -1)$  describes the phantom phase. By applying Eq.(38), we get

$$\omega_D = \frac{3(\sqrt{6}\alpha\sqrt{Q} + Q(\beta + 6\eta))}{6\alpha^2 + 2\sqrt{6}\alpha(\beta - 3)\sqrt{Q} + (\beta - 6)\beta Q}. \quad (53)$$

In terms of the redshift function, we have

$$\omega_D = \frac{3\alpha\sqrt{H_0^2\mathcal{U}^{2q+2}} + 3H_0^2(\beta + 6\eta)\mathcal{U}^{2q+2}}{(\alpha + (\beta - 6)\sqrt{H_0^2\mathcal{U}^{2q+2}})(\alpha + \beta\sqrt{H_0^2\mathcal{U}^{2q+2}})}. \quad (54)$$

Figure 3 shows the behavior of the *EoS* in the *GGDE*  $f(Q, L_m)$  theory for distinct parametric values. This plot indicates that the *EoS* parameter demonstrates a phantom regime, signifying that the cosmos is undergoing accelerated cosmic expansion.

### 3.2 Examination of $(\omega_D - \omega'_D)$ -Plane

Here, we employ  $(\omega_D - \omega'_D)$  analysis to examine the dynamics of *DE*. This analysis elucidates the impact of the modified terms on the deceleration parameter and the transition among various cosmic phases. The dynamics of

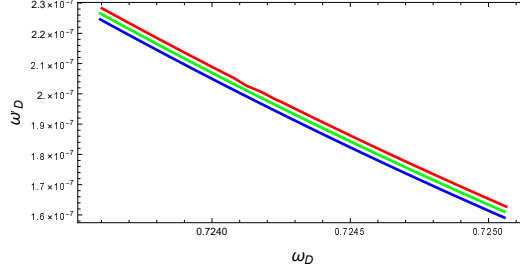


Figure 4: Plot of  $\omega_D$  versus  $\omega'_D$  for  $\alpha = 1.5$ ,  $\beta = 6.5$  and  $c_1 = 0.4$ .

*DE* with the scalar field has been studied in [64]. Caldwell and Linder [65] classified *DE* frameworks into two different categories, i.e., the thawing region and the freezing region. In the thawing region, the cosmic acceleration happens over a short period which is characterized by the positive value of  $\omega'_D$  and negative value of  $\omega_D$ . Whereas, the cosmic acceleration happens over a long period in the frozen region, defined by negative value of  $\omega'_D$  and positive value of  $\omega_D$ . In the  $(\omega_D - \omega'_D)$  plane, the standard model is expressed by the point  $(-1, 0)$ . Using Eq.(53), we have

$$\omega'_D = \frac{3\alpha(6\sqrt{6}\alpha^2 + 12\alpha\sqrt{Q}(\beta + 6\eta) + \sqrt{6}Q(\beta^2 + 12(\beta - 3)\eta))}{2\sqrt{Q}(6\alpha^2 + 2\sqrt{6}\alpha(\beta - 3)\sqrt{Q} + (\beta - 6)\beta Q)^2}. \quad (55)$$

This relation in terms of redshift function turns out to be

$$\omega'_D = \frac{\alpha(\alpha + 2(\beta + 6\eta)\sqrt{H_0^2\mathcal{U}^{2q+2}}) + H_0^2(\beta^2 + 12(\beta - 3)\eta)\mathcal{U}^{2q+2}}{4\sqrt{H_0^2\mathcal{U}^{2q+2}}(\alpha(\alpha + 2(\beta - 3)\sqrt{H_0^2\mathcal{U}^{2q+2}}) + (\beta - 6)\beta H_0^2\mathcal{U}^{2q+2})^2}. \quad (56)$$

Figure 4 exhibits that the values of  $\omega_D$  and  $\omega'_D$  are in 0 and 1. This behavior corresponds to the standard model, indicating that cosmic expansion is undergoing a more accelerated rate in this framework.

### 3.3 Investigation of $r - s$ Plane

The  $r - s$  parameters offer a more detailed comprehension of the dynamical behavior and evolutionary phases of *DE* models [66]. These operators delineate the distinctions across diverse cosmological models and also provide the distance of a specific model through the lambda *CDM* limit. These two dimensionless parameters characterize the standard model at  $(r, s) = (1, 1)$  and *CDM* model at  $(r, s) = (1, 0)$ . Furthermore, when the trajectories of



the  $(r - s)$  plane fall in the interval of  $(r < 1, s > 0)$ , one can experience the phantom and quintessence cosmic eras. Conversely, the Chaplygin gas model is obtained for  $r > 1$  and  $s < 0$ . These are classified as [67]

$$\begin{aligned} r &= \frac{\ddot{a}}{aH^3} = 1 + \frac{9\omega_D}{2}\Omega_D(1 + \omega_D) - \frac{3\omega'_D}{2H}\Omega_D \\ s &= \frac{r - 1}{3(q - \frac{1}{2})} = 1 + \omega_D - \frac{\omega'_D}{3\omega_D H}. \end{aligned} \quad (57)$$

Substituting the values of  $\omega_D$  and  $\omega'_D$ , we obtain

$$\begin{aligned} r &= (-54\sqrt{6}\alpha^4 + 9\alpha Q^{3/2}(44\alpha^3 - \beta^3 - 12(\beta - 3)\beta\eta) + 18\alpha^2 Q^{5/2}(\beta(22\beta \\ &+ 54\eta - 51) + 24) + \beta Q^{7/2}(11\beta^3 + \beta^2(54\eta - 51) + 72\beta + 972\eta^2) \\ &+ \sqrt{6}\alpha Q^3(44\beta^3 + 9\beta^2(18\eta - 17) + 144\beta + 972\eta^2 + 6\sqrt{6}\alpha^3 Q^2(44\beta \\ &+ 54\eta - 51) - 162\alpha^3 \sqrt{Q}(\beta + 4\eta) - 27\sqrt{6}\alpha^2 Q(\beta^2 + 8\beta\eta - 12\eta))) \\ &\times (2Q^{3/2}(6\alpha^2 + 2\sqrt{6}\alpha(\beta - 3)\sqrt{Q} + (\beta - 6)\beta Q)^2)^{-1}, \quad (58) \\ s &= (-6\alpha^3 + 6\sqrt{6}\alpha^3 Q^{3/2} + 3\sqrt{6}\alpha\beta Q^{5/2}(\beta + 4\eta - 2) + Q^3(\beta + 6\eta) \\ &\times ((\beta - 3)\beta + 18\eta) + 18\alpha^2 Q^2(\beta + 2\eta - 1) - 2\sqrt{6}\alpha^2 \sqrt{Q}(\beta + 6\eta) \\ &- \alpha Q(\beta^2 + 12(\beta - 3)\eta))(Q^{3/2}(6\alpha^2 + 2\sqrt{6}\alpha(\beta - 3)\sqrt{Q} + (\beta - 6)\beta Q) \\ &\times (\sqrt{6}\alpha + \sqrt{Q}(\beta + 6\eta)))^{-1}. \quad (59) \end{aligned}$$

These parameters in terms of the redshift function are

$$\begin{aligned} r &= (-\alpha^4 + \alpha(44\alpha^3 - \beta^3 - 12(\beta - 3)\beta\eta)(H_0^2 \mathcal{U}^{2q+2})^{3/2} - 3\alpha^3(\beta + 4\eta) \\ &\times \sqrt{H_0^2 \mathcal{U}^{2q+2} + 4\alpha^3 H_0^4(44\beta + 54\eta - 51)\mathcal{U}^{4q+4} - 3\alpha^2 H_0^2(\beta^2 + 8\beta\eta \\ &- 12\eta)\mathcal{U}^{2q+2} + 12\alpha^2(\beta(22\beta + 54\eta - 51) + 24)(H_0^2 \mathcal{U}^{2q+2})^{5/2} \\ &+ 4\alpha H_0^6(44\beta^3 + 9\beta^2(18\eta - 17) + 144\beta + 972\eta^2)\mathcal{U}^{6q+6} + 4\beta(11\beta^3 \\ &+ \beta^2(54\eta - 51) + 72\beta + 972\eta^2)(H_0^2 \mathcal{U}^{2q+2})^{7/2})(8(H_0^2 \mathcal{U}^{2q+2})^{3/2} \\ &\times (\alpha(\alpha + 2(\beta - 3)\sqrt{H_0^2 \mathcal{U}^{2q+2}} + (\beta - 6)\beta H_0^2 \mathcal{U}^{2q+2}))^2)^{-1} \quad (60) \\ s &= (\alpha H_0^2 \mathcal{U}^{2q+2}(36(\eta + \alpha^2 \sqrt{H_0^2 \mathcal{U}^{2q+2}}) - \beta(\beta + 12\eta)) - \alpha^2(\alpha \\ &+ 2(\beta + 6\eta)\sqrt{H_0^2 \mathcal{U}^{2q+2}}) + 108\alpha H_0^4 \mathcal{U}^{4q+4}(\alpha(\beta + 2\eta - 1) \\ &+ \beta(\beta + 4\eta - 2)\sqrt{H_0^2 \mathcal{U}^{2q+2}}) + 36H_0^6(\beta + 6\eta)((\beta - 3)\beta + 18\eta) \end{aligned}$$

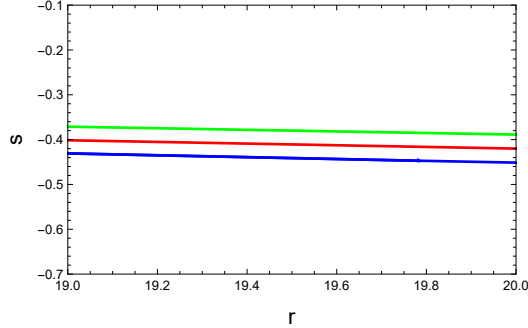


Figure 5: Plot of  $r$  against  $s$  corresponding to  $\alpha = 1.5$ ,  $\beta = 6.5$  and  $c_1 = 0.4$ .

$$\begin{aligned}
& \times \mathcal{U}^{6q+6})(36(H_0^2\mathcal{U}^{2q+2})^{3/2}(\alpha(\alpha + 2(\beta - 3)\sqrt{H_0^2\mathcal{U}^{2q+2}})) \\
& + (\beta - 6)\beta H_0^2\mathcal{U}^{2q+2})(\alpha + (\beta + 6\eta)\sqrt{H_0^2\mathcal{U}^{2q+2}})^{-1}. \tag{61}
\end{aligned}$$

Figure 5 demonstrates that  $r > 1$  and  $s < 0$ , indicating the Chaplygin gas model.

### 3.4 Stability Analysis

In the realm of modified gravity theories, stability analysis plays a crucial role in determining the physical viability of any cosmological model. A critical aspect of this investigation is to ensure that the model remains stable under small perturbations, thus avoiding instabilities. One key parameter in this analysis is the squared sound speed ( $v_s^2$ ), which characterizes the propagation of perturbations in the cosmic fluid. A physically viable model must maintain  $v_s^2 \geq 0$  to avoid the irregularities, which lead to instabilities such as growing perturbations or shock waves. In the background of  $f(Q, L_m)$  combined with *GGDE* model, the interaction between matter, non-metricity and *GGDE* introduce new terms affecting ( $v_s^2$ ), making it crucial to ensure the model remains stable against perturbations. Stability analysis, including the behavior of the ( $v_s^2$ ), allows us to explore the ranges of model parameters where perturbations decay and the evolution remains physically consistent with cosmic observations. This analysis reveal whether the  $f(Q, L_m)$  along with *GGDE* model offers solutions that remain stable throughout the cosmic evolution, particularly during the transition from early cosmic inflation to the current accelerated expansion.

By ensuring the stability of this extended gravity framework, including the positivity of the  $(v_s^2)$ , we apply the model to address key cosmological questions, such as the nature of *GGDE*. This analysis not only solidifies the theoretical foundation of the  $f(Q, L_m)$  in the framework of *GGDE* but also positions it as a promising alternative to standard cosmology. This parameter is given by

$$\begin{aligned}
v_s^2 &= \frac{P'_D}{\mu'_D} = \frac{\mu_D}{\mu'_D} \omega'_D + \omega_D \\
&= (6\sqrt{Q}(36\alpha^4 + \sqrt{6}\alpha\beta Q^{3/2}(\beta(4\beta + 21\eta - 15) - 72\eta) + (\beta - 6)\beta^2 Q^2(\beta \\
&\quad + 6\eta) + 6\sqrt{6}\alpha^3 \sqrt{Q}(4\beta + 9\eta - 3) + 36\alpha^2 Q(\beta(\beta + 4\eta - 2) - 6\eta))) \\
&\quad \times ((\sqrt{6}\alpha + 2\beta\sqrt{Q})(6\alpha^2 + 2\sqrt{6}\alpha(\beta - 3)\sqrt{Q} + (\beta - 6)\beta Q)^2)^{-1}. \quad (62)
\end{aligned}$$

Substituting the value of non-metricity, we have

$$\begin{aligned}
v_s^2 &= (6\sqrt{H_0^2 \mathcal{U}^{2q+2}}(\alpha^3(\alpha + (4\beta + 9\eta - 3)\sqrt{H_0^2 \mathcal{U}^{2q+2}}) \\
&\quad + \alpha H_0^2 \mathcal{U}^{2q+2}(6\alpha(\beta(\beta + 4\eta - 2) - 6\eta) + \beta(\beta(4\beta + 21\eta - 15) \\
&\quad - 72\eta)\sqrt{H_0^2 \mathcal{U}^{2q+2}}) + (\beta - 6)\beta^2 H_0^4 (\beta + 6\eta)\mathcal{U}^{4q+4})) \\
&\quad \times ((\alpha + 2\beta\sqrt{H_0^2 \mathcal{U}^{2q+2}})(\alpha(\alpha + 2(\beta - 3) \\
&\quad \times \sqrt{H_0^2 \mathcal{U}^{2q+2}} + (\beta - 6)\beta H_0^2 \mathcal{U}^{2q+2}))^2)^{-1}. \quad (63)
\end{aligned}$$

Figure 6 demonstrates that the  $(v_s^2) > 0$  in the framework of  $f(Q, L_m)$  gravity for the *GGDE* model. This result is significant for the viability and robustness of the model as it indicates that the model remains well-behaved under perturbations and aligns with fundamental stability criteria in cosmological evolution. In this context, the  $f(Q, L_m)$  combined with *GGDE* model offers an enriched framework, potentially explaining the cosmic accelerated expansion. The stability provided by  $v_s^2 > 0$  reinforces the model capacity to address large-scale cosmological observations while maintaining internal consistency. This analysis not only affirms the stability of the cosmic evolution for the *GGDE* model but also supports the broader applicability of the model in explaining key features of the universe expansion. The stable propagation of perturbations indicates that the model can be used to explore a wide range of cosmological phenomena from early universe inflation to late-time cosmic acceleration, offering valuable insights into the interaction between *DE* and

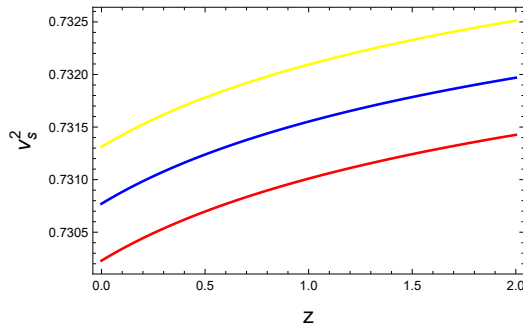


Figure 6: Graph of squared sound speed versus redshift function for  $\alpha = 1.5$ ,  $\beta = 6.5$  and  $c_1 = 0.4$ .

modified gravity. Thus, the positivity of the squared sound speed serves as a cornerstone for the reliability and physical applicability.

## 4 Summary and Discussion

The reconstruction process in modified theory provides a useful mechanism for developing a feasible  $DE$  model, capable of precisely predicting the trajectory of cosmic evolution. The main objective to explore a modified  $f(Q, L_m)$  theory stems from numerous critical reasons pertaining to both theoretical and observational frameworks in cosmology and gravitational physics. This modified framework explains the cosmic acceleration without the need for a cosmological constant. The structure of the  $f(Q, L_m)$  theory is inspired by other established modified theories. The combination of non-metricity and the matter-source term facilitates the development of a geometrically coherent theory that preserves essential phenomenological advantages, including the elucidation of late-time acceleration and producing viable inflationary models. Thus, this alternative theory aims to transcend the constraints of  $GR$  to address cosmological singularities and investigate innovative geometric structures via non-metricity, offering a cohesive explanation for  $DE$ ,  $DM$  and cosmic inflation. The inclusion of the matter-source term enriches the theoretical framework, offering new avenues for cosmological model building and consistency with current observations.

In this manuscript, we have explored the novel cosmological insights of  $f(Q, L_m)$  theory by considering  $GGDE$  model. The diagnostic tools and the statefinder pair are used to analyze the various eras of the cosmos. Further-

more, the model stability is evaluated using the squared sound speed method. The significant results are detailed below.

- The reconstructed  $GGDE$   $f(Q, L_m)$  gravity exhibits a rising trend corresponding to non-metricity and redshift function, signifying the realistic behavior of the model (Figure 1).
- The increasing behavior of energy density and decreasing pattern of pressure implies that the current cosmos is in a state of expansion (Figure 2).
- Our analysis also reveals that the  $EoS$  parameter describes the standard cosmic model, aligning with the observed behavior of the universe (Figure 3).
- The increasing trend in the  $(\omega_D - \omega'_D)$  plane indicates the freezing zone corresponding to different values of  $\eta$  (Figure 4). This suggests that  $GGDE$  theory results in the rapid expansion of the cosmos.
- The  $(r - s)$  plane demonstrates the Chaplygin gas model, indicating that the reconstructed functional form support the cosmic acceleration (Figure 5).
- Our findings indicate that the reconstructed  $GGDE$   $f(Q, L_m)$  gravity is stable as squared sound speed is positive (Figure 6).

The findings of our study significantly advance the understanding of  $DE$  models by providing a comprehensive framework that links  $GGDE$  with the extended  $f(Q, L_m)$  gravitational theory. By reconstructing the  $f(Q, L_m)$  model in the context of  $GGDE$ , our research reveals a nuanced interplay between non-metricity, matter sources and cosmic evolution. This approach offers a novel perspective on the theoretical underpinnings of dark energy, particularly by addressing limitations in the  $\Lambda$ CDM model. Unlike standard models, the reconstructed  $f(Q, L_m)$  framework incorporates both geometric and matter-Lagrangian terms, providing a more holistic depiction of the cosmos. Our findings demonstrate that the reconstructed  $GGDE$  model aligns well with recent observational data, reported by the Planck satellite and the Hubble parameter derived from CMB studies. Notably, the diagnostic tools such as the  $(\omega_D, \omega'_D)$ -plane and the  $(r, s)$ -plane, show that the model captures the freezing regime of  $DE$ , indicating of an accelerated expansion

phase consistent with observational data. Furthermore, the analysis of the energy density and pressure evolution underlines a phantom-like behavior, signifying a more rapid expansion of the cosmos and offering insights into possible late-time cosmic scenarios. These results provide robust evidence that the  $f(Q, L_m)$  framework is a viable alternative to  $DE$  models, offering compatibility with observational constraints while introducing new pathways to explore the dynamics of the dark universe. By bridging theoretical constructs with empirical data, this study not only enriches the field of modified gravity but also sets the stage for further exploration of non-metricity-driven cosmic phenomena, making a substantial contribution to understanding the nature of  $DE$  and the accelerated expansion of the universe.

The  $GGDE$   $f(Q, L_m)$  model has stable properties and consistently adheres to the current cosmic accelerated expansion. The phantom nature of the cosmos is observed to indicate a more rapid regime, potentially resulting in the current cosmic acceleration. The results align with the existing observational data given as [68]

- $\omega_D = -1.023^{+0.091}_{-0.096}$  (Planck TT+LowP+ext),
- $\omega_D = -1.006^{+0.085}_{-0.091}$  (Planck TT+LowP+lensing+ext),
- $\omega_D = -1.0019^{+0.075}_{-0.080}$  (Planck TT, TE, EE+LowP+ext).

The data has been obtained using various observational methods with a confidence level of 95%. Our findings align with the  $DE$  model in  $f(Q)$  [69] and  $f(Q, T)$  gravity [70]. It is worthwhile to highlight that our findings also align with the most recent data from theoretical observations [67]. Sharif and Zubair [71] delved into the evolution of pilgrim  $DE$  corresponding to event horizon, particle horizon and conformal age of the universe in the framework of the  $FRW$  universe but they did not check stability. We have also analyzed the stability of the system. Our findings are found to be more concise with observational data.

## Appendix $\mathcal{X}$ : Computation of $Q$

Using Eqs.(19) and (20), we obtain

$$Q \equiv -g^{\xi\eta}(L^\gamma_{\vartheta\xi}L^\vartheta_{\eta\gamma} - L^\gamma_{\vartheta\gamma}L^\vartheta_{\xi\eta}), \quad (\mathcal{X}1)$$

$$L^\gamma_{\vartheta\xi} = -\frac{1}{2}g^{\gamma\varepsilon}(Q_{\xi\vartheta\varepsilon} + Q_{\vartheta\varepsilon\xi} - Q_{\varepsilon\vartheta\xi}), \quad (\mathcal{X}2)$$

$$L^\vartheta_{\eta\gamma} = -\frac{1}{2}g^{\vartheta\psi}(Q_{\gamma\eta\psi} + Q_{\eta\gamma\psi} - Q_{\psi\eta\gamma}), \quad (\mathcal{X}3)$$

$$L^\gamma_{\vartheta\gamma} = -\frac{1}{2}g^{\gamma\psi}(Q_{\gamma\vartheta\psi} + Q_{\vartheta\psi\gamma} - Q_{\psi\gamma\vartheta}), \quad (\mathcal{X}4)$$

$$L^\vartheta_{\xi\eta} = -\frac{1}{2}g^{\vartheta\psi}(Q_{\eta\xi\psi} + Q_{\xi\psi\eta} - Q_{\psi\xi\eta}). \quad (\mathcal{X}5)$$

Therefore, we get

$$-g^{\xi\eta}L^\gamma_{\vartheta\xi}L^\vartheta_{\eta\gamma} = -\frac{1}{4}(2Q^{\gamma\eta\psi}Q_{\psi\gamma\eta} - Q^{\gamma\eta\psi}Q_{\gamma\eta\psi}), \quad (\mathcal{X}6)$$

$$g^{\xi\eta}L^\gamma_{\vartheta\gamma}L^\vartheta_{\xi\eta} = \frac{1}{4}g^{\xi\eta}g^{\vartheta\varepsilon}Q_\vartheta(Q_{\eta\xi\varepsilon} + Q_{\xi\varepsilon\eta} - Q_{\varepsilon\eta\xi}), \quad (\mathcal{X}7)$$

$$Q = -\frac{1}{4}(-Q^{\gamma\eta\xi}Q_{\gamma\eta\xi} + 2Q^{\gamma\eta\xi}Q_{\xi\gamma\eta} - 2Q^\gamma\tilde{Q}_\gamma + Q^\gamma Q_\gamma). \quad (\mathcal{X}8)$$

Using Eq.(23), we have

$$P^{\gamma\xi\eta} = \frac{1}{4}\left[-Q^{\gamma\xi\eta} + Q^{\xi\gamma\eta} + Q^{\eta\gamma\xi} + Q^\gamma g^{\xi\eta} - \tilde{Q}^\gamma g^{\xi\eta} - \frac{1}{2}(g^{\gamma\xi}Q^\eta + g^{\gamma\eta}Q^\xi)\right], \quad (\mathcal{X}9)$$

$$-Q_{\gamma\xi\eta}P^{\gamma\xi\eta} = -\frac{1}{4}(-Q^{\gamma\xi\eta}Q_{\gamma\xi\eta} + 2Q_{\gamma\xi\eta}Q^{\xi\gamma\eta} + Q^\gamma Q_\gamma - 2Q_\gamma\tilde{Q}^\gamma) = (\mathcal{X}10)$$

## Appendix $\mathcal{Y}$ : Variation of $Q$

We consider  $Q$  as

$$Q_{\gamma\xi\eta} = \nabla_\gamma g_{\xi\eta}, \quad (\mathcal{Y}1)$$

$$Q^\gamma_{\xi\eta} = g^{\gamma\vartheta}Q_{\vartheta\xi\eta} = g^{\gamma\vartheta}\nabla_\vartheta g_{\xi\eta} = \nabla^\gamma g_{\xi\eta}, \quad (\mathcal{Y}2)$$

$$Q_{\gamma\xi}^\eta = g^{\xi\vartheta}Q_{\gamma\vartheta\eta} = g^{\xi\vartheta}\nabla_\gamma g_{\vartheta\eta} = -g_{\vartheta\eta}\nabla_\gamma g^{\xi\vartheta}, \quad (\mathcal{Y}3)$$

$$Q_{\gamma\xi}^\eta = g^{\eta\vartheta}Q_{\gamma\xi\vartheta} = g^{\eta\vartheta}\nabla_\gamma g_{\xi\vartheta} = -g_{\xi\vartheta}\nabla_\gamma g^{\eta\vartheta}, \quad (\mathcal{Y}4)$$

$$Q_{\gamma\xi}^\eta = g^{\gamma\vartheta}g^{\xi\varepsilon}\nabla_\vartheta g_{\varepsilon\eta} = g^{\xi\varepsilon}\nabla^\gamma g_{\varepsilon\eta} = -g_{\varepsilon\eta}\nabla^\gamma g^{\xi\varepsilon}, \quad (\mathcal{Y}5)$$

$$Q_{\gamma\xi}^\eta = g^{\gamma\vartheta}g^{\eta\varepsilon}\nabla_\vartheta g_{\xi\varepsilon} = g^{\eta\varepsilon}\nabla^\gamma g_{\xi\varepsilon} = -g_{\xi\varepsilon}\nabla^\gamma g^{\eta\varepsilon}, \quad (\mathcal{Y}6)$$

$$Q_{\gamma\xi}^\eta = g^{\xi\varepsilon}g^{\eta\vartheta}\nabla_\gamma g_{\varepsilon\vartheta} = -g^{\xi\varepsilon}g_{\varepsilon\vartheta}\nabla_\gamma g^{\eta\vartheta} = -\nabla_\gamma g^{\xi\eta}, \quad (\mathcal{Y}7)$$

$$Q^{\gamma\xi\eta} = -\nabla^\gamma g_{\xi\eta}. \quad (\mathcal{Y}8)$$

Using Eqs.( $\mathcal{Y}6$ ) and ( $\mathcal{Y}7$ ), we obtain

$$\begin{aligned} \delta Q &= -\frac{1}{4}\delta\left(-Q^{\gamma\eta\xi}Q_{\gamma\eta\xi} + 2Q^{\gamma\eta\xi}Q_{\xi\gamma\eta} - 2Q^\gamma\tilde{Q}_\gamma + Q^\gamma Q_\gamma\right), \\ &= -\frac{1}{4}\left(-\delta Q^{\gamma\eta\xi}Q_{\gamma\eta\xi} - Q^{\gamma\eta\xi}\delta Q_{\gamma\eta\xi} + 2\delta Q^{\gamma\eta\xi}Q_{\xi\gamma\eta} \right. \\ &\quad \left. + 2Q^{\gamma\eta\xi}\delta Q_{\xi\gamma\eta} - 2\delta Q^\gamma\tilde{Q}_\gamma - 2Q^\gamma\delta\tilde{Q}_\gamma + \delta Q^\gamma Q_\gamma + Q^\gamma\delta Q_\gamma\right), \\ &= -\frac{1}{4}\left[Q_{\gamma\eta\xi}\nabla^\gamma\delta g^{\eta\xi} - Q^{\gamma\eta\xi}\nabla_\gamma\delta g_{\eta\xi} - 2Q_{\xi\gamma\eta}\nabla^\gamma\delta g^{\eta\xi} + 2Q^{\gamma\eta\xi}\nabla_\xi\delta g_{\gamma\eta} \right. \\ &\quad \left. + 2\tilde{Q}_\gamma\nabla^\gamma g^{\xi\eta}\delta g_{\xi\eta} + 2\tilde{Q}_\gamma g_{\xi\eta}\nabla^\gamma\delta g^{\xi\eta} - 2Q^\gamma\nabla^\vartheta\delta g_{\gamma\vartheta} - Q_\gamma\nabla^\gamma g^{\xi\eta}\delta g_{\xi\eta} \right. \\ &\quad \left. - Q_\gamma g_{\xi\eta}\nabla^\gamma\delta g^{\xi\eta} - Q^\gamma\nabla_\gamma g^{\xi\eta}\delta g_{\xi\eta} - Q^\gamma g_{\xi\eta}\nabla_\gamma\delta g^{\xi\eta}\right]. \quad (\mathcal{Y}9) \end{aligned}$$

Here, we use the following equations as

$$\delta g_{\xi\eta} = -g_{\xi\gamma}\delta g^{\gamma\vartheta}g_{\vartheta\eta}, \quad (\mathcal{Y}10)$$

$$\begin{aligned} -Q^{\gamma\eta\varepsilon}\nabla_\gamma\delta g_{\eta\varepsilon} &= -Q^{\gamma\eta\varepsilon}\nabla_\gamma(-g_{\eta\vartheta}\delta g^{\vartheta\vartheta}g_{\vartheta\varepsilon}) \\ &= 2Q^{\gamma\psi}_\eta Q_{\gamma\psi\varepsilon}\delta g^{\xi\eta} + Q_{\gamma\eta\varepsilon}\nabla^\gamma g^{\eta\varepsilon}, \quad (\mathcal{Y}11) \end{aligned}$$

$$2Q^{\gamma\eta\varepsilon}\nabla_\varepsilon\delta g_{\gamma\eta} = -4Q_\xi^{\psi\varepsilon}Q_{\varepsilon\psi\eta}\delta g^{\xi\eta} - 2Q_{\eta\varepsilon\gamma}\nabla^\gamma g^{\eta\varepsilon}, \quad (\mathcal{Y}12)$$

$$\begin{aligned} -2Q^\varepsilon\nabla^\vartheta\delta g_{\varepsilon\vartheta} &= 2Q^\gamma Q_{\eta\gamma\xi}\delta g^{\xi\eta} + 2Q_\xi\tilde{Q}_\eta\delta g^{\xi\eta} \\ &\quad + 2Q_\eta g_{\gamma\varepsilon}\nabla^\gamma g^{\eta\varepsilon}. \quad (\mathcal{Y}13) \end{aligned}$$

Thus, Eq.( $\mathcal{Y}9$ ) becomes

$$\delta Q = 2P_{\gamma\eta\varepsilon}\nabla^\gamma\delta g^{\eta\varepsilon} - (P_{\xi\gamma\vartheta}Q_\eta{}^{\gamma\vartheta} - 2Q^{\gamma\vartheta}_\xi P_{\gamma\vartheta\eta})\delta g^{\xi\eta}, \quad (\mathcal{Y}14)$$

where

$$\begin{aligned} 2P_{\gamma\eta\varepsilon} &= -\frac{1}{4}\left[2Q_{\gamma\eta\varepsilon} - 2Q_{\varepsilon\gamma\eta} - 2Q_{\eta\varepsilon\gamma} + 2Q_\eta g_{\gamma\varepsilon} \right. \\ &\quad \left. + 2(\tilde{Q}_\gamma - Q_\gamma)g_{\eta\varepsilon}\right], \quad (\mathcal{Y}15) \end{aligned}$$

$$4(P_{\xi\gamma\vartheta}Q_\eta{}^{\gamma\vartheta} - 2Q^{\gamma\vartheta}_\xi P_{\gamma\vartheta\eta}) = 2Q^{\gamma\vartheta}_\eta Q_{\gamma\vartheta\xi} - 4Q_\xi{}^{\gamma\vartheta}Q_{\vartheta\gamma\eta} + 2\tilde{Q}^\gamma Q_{\gamma\xi\eta}$$



$$+ 2Q^\gamma Q_{\eta\gamma\xi} + 2Q_\xi \tilde{Q}_\eta - Q^\gamma Q_{\gamma\xi\eta}. \quad (\mathcal{Y}16)$$

**Data Availability Statement:** The research presented in this paper did not utilize any data.

## References

- [1] Swaters, R.A. et al.: *Astrophys. J.* **531**(2000)107.
- [2] Sahni, V. and Starobinsky, A.A.: *Int. J. Mod. Phys. D* **9**(2000)373; Carroll, S.M.: *Living Rev. Rel.* **4**(2001)1.
- [3] Nojiri, S.I. and Odintsov, S.D.: *Int. J. Geom. Methods Mod. Phys.* **4**(2007)115.
- [4] Urban, F.R. and Zhitnitsky, A.R.: *Phys. Rev. D* **80**(2009)063001.
- [5] Ohta, N.: *Phys. Lett. B* **695**(2011)41.
- [6] Cai, R.G. et al.: *Phys. Rev. D* **84**(2011)123501.
- [7] Sheykhi, A. and Movahed, M.S.: *Gen. Relativ. Gravit.* **44**(2012)449.
- [8] Feng, C.J. et al.: *Mod. Phys. Lett. A* **27**(2012)1250182.
- [9] Hayashi, K. and Shirafuji, T.: *Phys. Rev. D* **19**(1979)3524.
- [10] Linder, E.V.: *Phys. Rev. D* **81**(2010)127301.
- [11] Jimenez, J.B. et al.: *Phys. Rev. D* **98**(2018)044048.
- [12] Adeel, M.: et al.: *Mod. Phys. Lett. A* **38**(2023)2350152.
- [13] Sharif, M.: et al.: *Chin. J. Phys.* **91**(2024)66.
- [14] Rani, S.: et al.: *Int. J. Geom. Methods Mod. Phys.* **21**(2024)2450033.
- [15] Gul, M.Z. et.: *Eur. Phys. J. C* **84**(2024)8.
- [16] Maurya, S.K. et al.: *Phys. Dark Universe* **46**(2024)101619.

- [17] Sharif, M.: et al.: *New Astron.* **109**(2024)102211.
- [18] Rani, S.: et al.: *Phys. Dark Universe* **47**(2025)101754.
- [19] Sharif, M.: et al.: *Phys. Dark Universe* **47**(2025)101760.
- [20] Zhadyranova, A.: *J. High Energy Astrophys.* **44**(2024)123.
- [21] Gul, M.Z. et al.: *Phys. Scr.* **99**(2024)045006.
- [22] Koussour, M.: *Chin. J. Phys.* **90**(2024)108.
- [23] Sharif, M. et al.: *Phys. Scr.* **99**(2024)115003.
- [24] Gul, M.Z. et al.: *Chin. Phys. C.* **48**(2024)12503.
- [25] Koussour, M.: *Phys. Dark Universe* **45**(2024)101527.
- [26] Gul, M.Z. et al.: *Chin. J. Phys.* **93**(2025)256.
- [27] Nan, G. et al.: *Phys. Dark Universe* **46**(2024)101635.
- [28] Gul, M.Z. et al.: *Eur. Phys. J. C* **84**(2024)775; *ibid* 802; *ibid* 1232.
- [29] Sharif, M. et al.: *Mod. Phys. Lett. A* **39**(2024)2450140.
- [30] Pradhan, S. et al.: *Fortschr. der Phys.* **72**(2024)2400092.
- [31] Gul, M.Z. et al.: *Gen. Relativ. Gravit.* **56**(2024)45.
- [32] Koussour, M. et al.: *Phys. Dark Universe* **46**(2024)101577.
- [33] Gul, M.Z. et al.: *Chin. J. Phys.* **88**(2024)388.
- [34] Sharif, M. et al.: *Eur. Phys. J. C* **84**(2024)1094.
- [35] Myrzakulov, Y. et al.: *Phys. Dark Universe* **45**(2024)101545.
- [36] Sharif, M. and Gul, M.Z.: *Ann. Phys.* **465**(2024)169674.
- [37] Errehymy, A. et al.: *Physics of the Dark Universe* **46**(2024)101555.
- [38] Sharif, M. and Gul, M.Z.: *Phys. Scr.* **99**(2024)065036.
- [39] Gul, M.Z. et al.: *Chin. J. Phys.* **89**(2024)1347.

- [40] Myrzakulov, Y. et al.: Phys. Dark Universe **46**(2024)101614.
- [41] Harko, T. et al.: Phys. Rev. D **98**(2018)084043.
- [42] Mandal, S. and Sahoo, P.K.: Phys. Lett. B **823**(2021)136786.
- [43] Myrzakulov, K.: J. High Energy Astrophys. **44**(2024)164.
- [44] Turner, M.S. and White M.: Phys. Rev. D **56**(1997)R4439.
- [45] Sahni, V. and Starobinsky, A.: Int. J. Mod. Phys. D **15**(2006)2105.
- [46] Chirde, V.R. and Shekh, S.H.: Astron. Astrophys. **58**(2015)106.
- [47] Arora, S. et al.: Phys. Dark Universe. **30**(2020)100664.
- [48] Solanki, R. et al.: Phys. Dark Universe. **36**(2022)100996.
- [49] Mussatayeva, A. et al.: Phys. Dark Universe. **42**(2023)101276.
- [50] Ebrahimi, E. and Sheykhi, A.: Phys. Lett. B **706**(2011)19.
- [51] Saaidi, K. et al.: Int. J. Mod. Phys. D **21**(2012)1250057.
- [52] Jawad, A.: Astrophys. Space Sci. **356**(2015)119.
- [53] Fayaz, V. et al.: Eur. Phys. J. Plus **131**(2016)22.
- [54] Sharif, M. and Nawazish, I.: Int. J. Mod. Phys. D **27**(2018)1850091.
- [55] Saridakis, E.N. et al.: J. Cosmol. Astropart. Phys. **2018**(2018)012.
- [56] Zadeh, M.A., Sheykhi, A., Moradpour, H. and Bamba, K.: Eur. Phys. J. C **78**(2018)11.
- [57] Ghaffari, S. et al.: Eur. Phys. J. C **78**(2018)706.
- [58] Huang, Q. et al.: Class. Quantum Grav. **36**(2019)175001.
- [59] Odintsov, S.D., Oikonomou, V.K. and Banerjee, S.: Nucl. Phys. B **938**(2019)935.
- [60] Myrzakulov, N. et al.: Front. Astron. Space Sci. **9**(2022)902552.

- [61] Sharif, M., Gul, M.Z. and Hashim, I.: Phys. Dark Universe **46**(2024)101606.
- [62] Sharif, M., Gul, M.Z. and Hashim, I.: Chin. J. Phys. **89**(2024)266.
- [63] Gul, M.Z., Sharif, M. and Hashim, I.: Phys. Dark Universe **45**(2024)101537.
- [64] Gadbail, G.N., Mandal, S. and Sahoo, P.K.: Physics **4**(2022)1403.
- [65] Caldwell, R.R. and Linder, E.V.: Phys. Rev. Lett. **95**(2005)141301.
- [66] Sahni, V. et al.: J. Exp. Theor. Phys. Lett. **77**(2003)201.
- [67] Myrzakulov, N.: Front. Astron. Space Sci. **9**(2022)902552.
- [68] Ade, P.A. et al.: Astron. Astrophys. **594**(2016)13.
- [69] Sharif, M. and Ajmal, M.: Chin. J. Phys. **88**(2024)706.
- [70] Sharif, M. and Ibrar, I.: Eur. Phys. J. Plus **139**(2024)17.
- [71] Sharif, M. and Zubair, M.: Astrophys. Space Sci. **353**(2014)699.